Since January 2020 Elsevier has created a COVID-19 resource centre with free information in English and Mandarin on the novel coronavirus COVID-19. The COVID-19 resource centre is hosted on Elsevier Connect, the company's public news and information website.

Virology 381 (2008) 215–221

Contents lists available at ScienceDirect

Virology

journal homepage: www.elsevier.com/locate/yviro

Importance of cholesterol-rich membrane microdomains in the interaction of the S protein of SARS-coronavirus with the cellular receptor angiotensin-converting enzyme 2

Joerg Glende [a,*], Christel Schwegmann-Wessels [a], Marwan Al-Falah [b], Susanne Pfefferle [c], Xiuxia Qu [d], Hongkui Deng [d], Christian Drosten [c,1], Hassan Y. Naim [b], Georg Herrler [a]

[a] Institut für Virologie, Stiftung Tierärztliche Hochschule Hannover, 30559 Hannover, Germany
[b] Institut für Physiologische Chemie der Stiftung Tierärztliche Hochschule Hannover, 30559 Hannover, Germany
[c] Bernhard-Nocht-Institut für Tropenmedizin, 20359 Hamburg, Germany
[d] Department of Cell Biology and Genetics, College of Life Sciences, Peking University, Beijing 100871, PR China

ARTICLE INFO

Article history:
Received 27 May 2008
Returned to author for revision 12 June 2008
Accepted 17 August 2008
Available online 23 September 2008

Keywords:
Cholesterol
Entry
Binding
SARS-CoV
Coronavirus
Lipid rafts

ABSTRACT

Cholesterol present in the plasma membrane of target cells has been shown to be important for the infection by SARS-CoV. We show that cholesterol depletion by treatment with methyl-β-cyclodextrin (mβCD) affects infection by SARS-CoV to the same extent as infection by vesicular stomatitis virus-based pseudotypes containing the surface glycoprotein S of SARS-CoV (VSV-ΔG-S). Therefore, the role of cholesterol for SARS-CoV infection can be assigned to the S protein and is unaffected by other coronavirus proteins. There have been contradictory reports whether or not angiotensin-converting enzyme 2 (ACE2), the cellular receptor for SARS-CoV, is present in detergent-resistant membrane domains. We found that ACE2 of both Vero E6 and Caco-2 cells co-purifies with marker proteins of detergent-resistant membranes supporting the notion that cholesterol-rich microdomains provide a platform facilitating the efficient interaction of the S protein with the cellular receptor ACE2. To understand the involvement of cholesterol in the initial steps of the viral life cycle, we applied a cell-based binding assay with cells expressing the S protein and cells containing angiotensin-converting enzyme 2 (ACE2). Alternatively, we used a soluble S protein as interaction partner. Depletion of cholesterol from the ACE2-expressing cells reduced the binding of S-expressing cells by 50% whereas the binding of soluble S protein was not affected. This result suggests that optimal infection requires a multivalent interaction between viral attachment protein and cellular receptors.

Introduction

Cellular infection by enveloped viruses proceeds via (i) the interaction of viral surface proteins with cell surface receptors to achieve the attachment of virus particles to the cell surface and (ii) the initiation of a fusion event that is usually triggered by a conformational change of a fusion protein (reviewed by Marsh and Helenius, 2006). Other features of this process vary between different groups of viruses. The viral membrane may fuse with either the plasma membrane or, upon endocytotic uptake of the virion, with the endosomal membrane. For many viruses the fusion protein has to be cleaved into subunits which may occur during transport to the plasma membrane or after virus release from the cell (Garten and Klenk, 1999). Another variant is the involvement of membrane microdomains in the fusion process (Chazal and Gerlier, 2003).

Within a membrane, sphingolipids and cholesterol form microdomains with an increased structural order (reviewed by Simons and Ikonen, 1997). Cholesterol maintains the tight packaging of the sphingolipids with their saturated fatty acid chains. Some proteins partition into these microdomains while others are excluded from them. The tight packaging of the lipid components renders the proteins resistant to solubilization by non-ionic detergents at 4 °C. Depletion of cholesterol from the membrane by drugs – e.g. by methyl-β-cyclodextrin (mβCD) – abolishes the detergent resistance. Pretreatment of cells with mβCD has revealed that viruses differ in their dependence on cholesterol for initiation of infection. For several viruses, e.g. *Human immunodeficiency virus*, *Murine leukemia virus* and *Herpes simplex virus*, it has been shown that they are sensitive to a reduction of the cholesterol content in the plasma membrane (Liao et al., 2001; Lu et al., 2002; Bender et al., 2003). For some viruses – influenza viruses and *Canine distemper virus* – cholesterol-enriched microdomains appear to be important in the viral membrane, but not

* Corresponding author. Fax: +49 511 953 8898.
E-mail address: joerg.glende@tiho-hannover.de (J. Glende).
[1] Present address: Institut für Virologie am Universitätsklinikum Bonn, Medizinische Fakultät, 53127 Bonn, Germany.

0042-6822/$ – see front matter © 2008 Elsevier Inc. All rights reserved.
doi:10.1016/j.virol.2008.08.026

in the cellular membrane (Sieczkarski and Whittaker, 2002; Imhoff et al., 2007). On the other hand, *Vesicular stomatitis virus* does not show a decreased infectivity after depletion of cholesterol from either the viral or cellular membrane (Popik et al., 2002; Imhoff et al., 2007).

Coronaviruses are enveloped viruses with a positive-stranded RNA genome (reviewed by Enjuanes et al., 2006). Three viral proteins are incorporated into the viral membrane, the M, E and S proteins. The latter plays an important role in the initiation of infection. For several coronaviruses, *Murine hepatitis virus*, *Infectious bronchitis virus*, human coronavirus 229E and SARS-CoV, it has been shown that cholesterol depletion from the plasma membrane of the target cells reduces the efficiency of infection (Nomura et al., 2004; Thorp and Gallagher, 2004; Choi et al., 2005; Imhoff et al., 2007; Li et al., 2007).

For SARS-CoV, the cholesterol dependence has been shown either with infectious virus or with viral pseudotypes. However, the explanation of the results is difficult because there are two reports that the cellular receptor for SARS-CoV, angiotensin-converting enzyme 2 (ACE2) is not present in detergent-resistant membrane domains but rather in the detergent-soluble fraction. Warner et al. (2005) obtained this result for CHO cells transiently expressing ACE2 and Li et al. (2007) for endogenous ACE2 of Vero E6 cells. By contrast, Lu et al. (2008) recently identified ACE2 as a raft protein similar to caveolin-1. So far there was no experimental indication whether cholesterol is required for binding of the virus to the cell surface or for the subsequent fusion event.

To clarify the points raised above, here we show that the cholesterol depletion and replenishment affects the infection efficiency of SARS-CoV to the same extent as that of pseudotypes containing the S protein of SARS-CoV. Furthermore, we show that ACE2 is present in detergent-resistant membranes of both Vero E6 cells and Caco-2 cells. Finally, we provide evidence that in a cell-based binding assay, cholesterol depletion affects the interaction of the S protein with ACE2.

Results

S-protein-mediated entry by SARS-CoV is cholesterol-dependent

For our studies on the importance of cholesterol in the initiation of an infection by SARS-CoV, we used viral pseudotypes based on replication-deficient VSV containing the S protein of SARS-CoV (VSV-ΔG-S). This approach allowed us to determine whether the cholesterol dependence of SARS-CoV entry that has been reported recently (Li et al., 2007) can be assigned solely to the S protein or whether it is dependent on additional coronavirus proteins. As control viruses we used pseudotypes containing the G protein (VSV-ΔG-G) of VSV that is unaffected by cholesterol depletion (Popik et al., 2002; Imhoff et al., 2007) and *Infectious bronchitis virus* (IBV), an avian coronavirus that has recently been shown to be sensitive to reduction of the cholesterol content in the plasma membrane of the target cell (Imhoff et al., 2007).

To investigate the involvement of cholesterol and a possible role of lipid rafts during the initial steps of a SARS-CoV infection, we used methyl-β-cyclodextrin (mβCD) to deplete cholesterol from target cells. MβCD is known to capture cholesterol and thereby sequestering cholesterol from the plasma membrane. As a result, lipid microdomains are disrupted and biological processes that depend on them are blocked. First, we determined the effect of mβCD treatment on the cholesterol content of Vero CCL-81 cells. These cells were used because in contrast to Vero E6 cells that are commonly used for propagation of SARS-CoV, the CCL-81 subline is sensitive to our control virus IBV. Using a fluorometric method based on an enzyme-coupled reaction that detects both free cholesterol and cholesteryl esters we found that incubation with increasing amounts of mβCD resulted in a decrease of the cholesterol levels in Vero cells. At an mβCD concentration of 10 mM, the concentration of cholesterol was reduced by about 50% (data not shown). To exclude that mβCD treatment has toxic effects we analyzed the viability of the cells after drug exposure. Up to a concentration of 10 mM mβCD, the cells exhibited viability rates comparable to that of untreated cells (data not shown).

To analyze whether cholesterol depletion affects entry mediated by the SARS-CoV S protein, we pretreated Vero CCL-81 cells with mβCD for 30 min and – after three washing steps – infected the cells by either VSV-ΔG-S pseudotypes or the control viruses VSV-ΔG-G and IBV, respectively. At 8 h p.i., the infectivity was determined by counting the fluorescent cells. In the case of pseudotype-infected cells, fluorescence was derived from eGFP expressed from the VSV genome. IBV-infected cells were visualized by immunostaining. As shown in Fig. 1A, mβCD treatment inhibited the infection by VSV-ΔG-S in a dose-dependent fashion. At mβCD concentrations of 2.5 mM and 10 mM, the percentage of infected cells was reduced by about 20% and 50%, respectively, compared to the untreated cells. For the infection by *Vesicular stomatitis virus* (VSV) or VSV-G-pseudotyped viruses, it has been reported that virus entry is not affected by depletion of cellular cholesterol (Popik et al., 2002; Thorp and Gallagher, 2004; Imhoff et al., 2007). We confirmed these results with our pseudotype system (Fig. 1A). For *Infectious bronchitis virus* (IBV), an avian coronavirus, it has been demonstrated that the infection is dependent on cellular cholesterol (Imhoff et al., 2007). Consistent with these data, IBV infection of cholesterol-depleted cells resulted in a decreased number of infected cells (Fig. 1A). At an mβCD concentration of 10 mM, the infection was reduced by about 40%. To assess whether the effect of

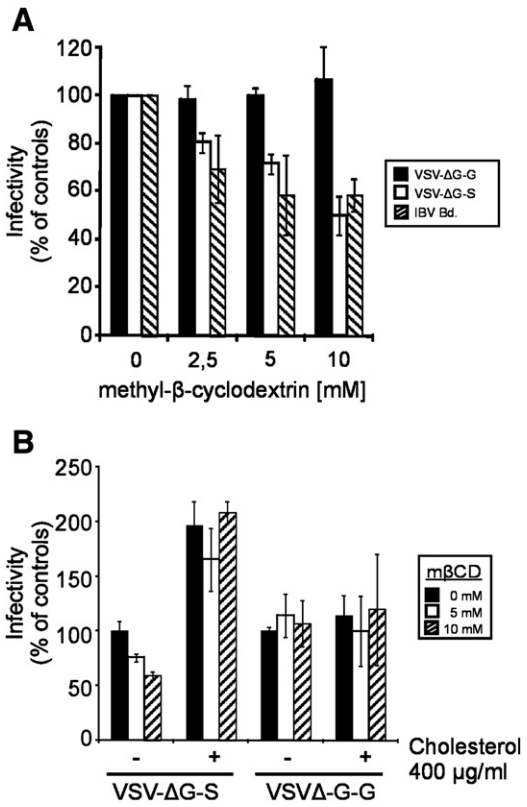

Fig. 1. Effect of cholesterol depletion and replenishment on virus infection. (A) Vero CCL-81 cells were treated with different mβCD concentrations. After removal of mβCD by three washing steps, cells were infected by VSV-ΔG-S (white bars) and the control viruses VSVΔG-G (black bars) and IBV (hatched bars). At 8 h p.i. cells were fixed. Infection was determined by counting eGFP-expressing (VSV-ΔG viruses) or by immunostaining (IBV). (B) Untreated and mβCD-treated Vero cells were incubated in the absence (−) or presence (+) of water-soluble cholesterol diluted in medium followed by infection with VSV-ΔG pseudotype viruses. Infectivity rates were determined as described for 1A. Each bar represents the mean±standard deviation of 3 independent experiments.

mβCD is reversible we used exogenous cholesterol to replenish the cholesterol-depleted cellular membranes and analyzed the recovery of virus infection. As shown in Fig. 1B, the addition of cholesterol reversed the inhibitory effect of mβCD on VSV-ΔG-S infection. In fact, infection rates even exceeded the values determined for cells that had not been treated with mβCD. The infectivity of VSV-ΔG-G was not affected by cholesterol supplementation.

To find out how the cholesterol dependence of the pseudotype infection relates to infection by SARS-CoV, Vero E6 cells were treated with 10 mM mβCD for 30 min at 37 °C followed by the infection with SARS-CoV at a multiplicity of infection (MOI) of about 0.0005. After the adsorption period, cells were overlaid by methylcellulose and incubated for 96 h for plaque formation to occur. As shown in Fig. 2, compared to untreated control cells the infectivity in cholesterol-depleted cells was reduced by about 60% at 10 mM mβCD treatment. This result is comparable to that obtained with pseudotype virus containing the S protein of SARS-CoV (Fig. 1A). We also included a control in which exogenous cholesterol (100 μg/ml) was added to mβCD-treated Vero cells for 30 min prior to infection with SARS-CoV. Under these conditions of cholesterol replenishment the inhibitory effect was abolished (Fig. 2). Our data confirm that cholesterol plays a critical role in SARS-CoV entry and demonstrate that the cholesterol dependence is a feature of the S protein and independent of other coronavirus proteins.

Role of cholesterol in binding of spike protein to ACE2

We analyzed the amount of ACE2 expressed on the cell surface after mβCD treatment and we found that cholesterol depletion did not affect the surface expression level of the SARS-CoV receptor (data not shown). This is in contrast to a recent report that cholesterol depletion results in a decreased expression level of ACE2 (Li et al., 2007). Possible reasons for this discrepancy will be discussed in a later section. To understand by what mechanism cholesterol depletion inhibits virus entry and to define the molecular step at which the inhibition occurs we established a cell-based binding assay as well as a binding assay with a soluble spike protein fused to human Fc. For the cell-based binding assay we generated a cell line derived from baby hamster kidney cells (BHK21) that constitutively expresses the SARS-CoV spike glycoprotein (BHK-SΔ18). To monitor the amount of cells that bind to ACE2-expressing Vero E6 cells, we applied the fluorescent fatty acid dye BODIPY FL C_{12} that incorporates into the plasma membrane. Fluorescent dye-labeled BHK-SΔ18 cells were resuspended in serum-free culture medium and added to a Vero E6 monolayer in a ratio of 1/2 (BHK-SΔ18 cells/Vero E6 cells). Unbound cells were removed by washing with PBS containing 0.5 M sodium chloride. As shown in Fig. 3A (panels c and d), BHK cells expressing the S protein of SARS-CoV bound efficiently to Vero E6 cells, whereas only a few cells of the parental BHK cells were detected (panels g and h).

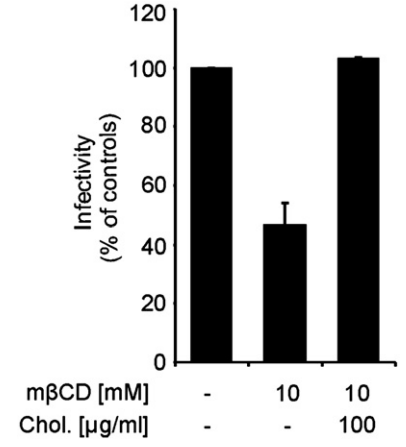

Fig. 2. Effect of cholesterol depletion/replenishment on SARS-CoV replication. Untreated, mβCD-treated and cholesterol replenished Vero cells were infected by SARS-CoV and overlaid with methylcellulose. At 96 h p.i., the cells were stained and the plaques were counted. The bars represent the mean values ± standard deviation of 3 independent experiments.

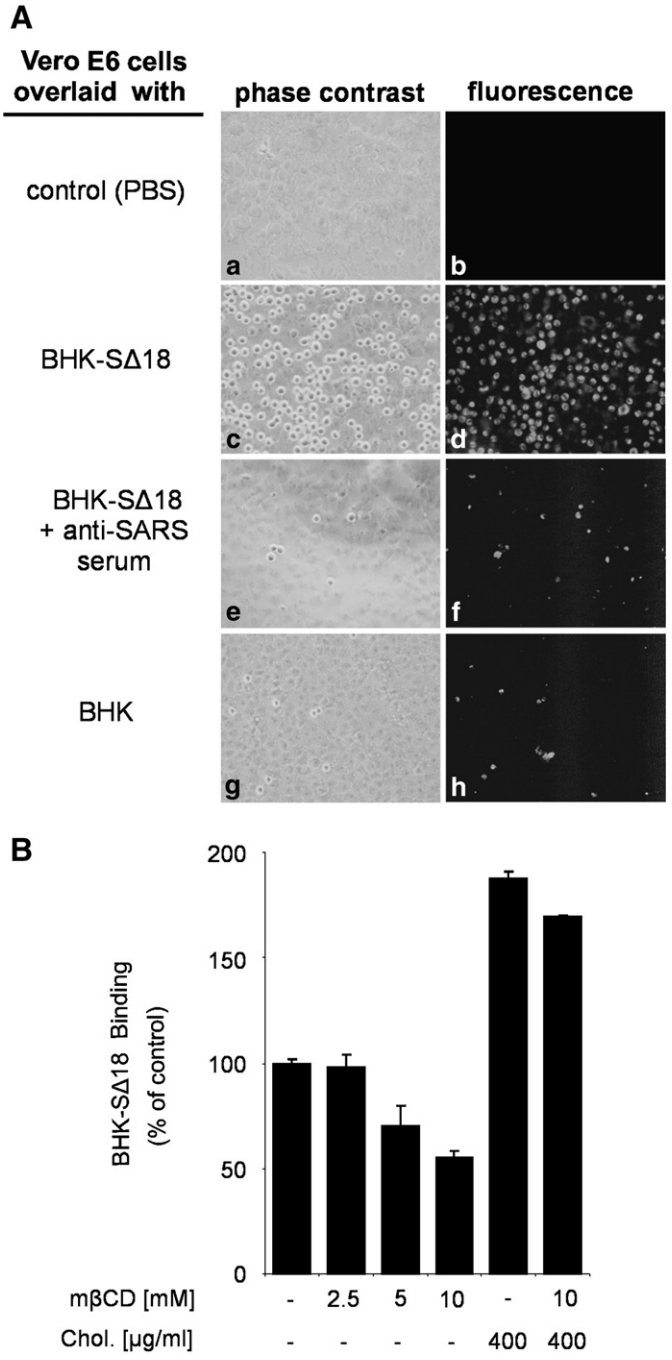

Fig. 3. Cell-based binding assay for the interaction of S protein with ACE2. BHK-SΔ18 cells were grown to monolayers in the presence of the fluorescent fatty acid BODIPY FL C_{12}. After detachment by treatment with Accutase, cells were used for overlay assays. (A) Confluent Vero E6 cells were overlaid with PBS (a and b), BHK-SΔ18 (c and d), BHK-SΔ18 that had been pretreated with anti-SARS serum (e and f), or with fluorescence-labeled BHK21 cells (g and h). Phase-contrast pictures are shown in panels on the left side (a, c, e, g); pictures obtained by fluorescence microscopy are shown on the right (b, d, f, h). (B) Confluent Vero E6 cells were treated with different concentrations of mβCD. In cholesterol replenishment experiments, cells were incubated in the presence of cholesterol. After these treatments, fluorescence-labeled BHK-SΔ18 cells were added. Bound cells were detached by trypsin treatment and subjected to flow cytometry. The figures show a representative image. The bars represent the mean ± standard deviation of 4 independent experiments.

Pretreatment of BHK-SΔ18 cells with a rabbit serum directed against SARS-CoV reduced the binding to a level comparable to that of BHK cells, i.e. about 3% (compare panels e and f with panels g and h). To address the question whether in our assay S protein interacts with ACE2 or another cellular protein, we performed the binding assay with three Vero cell lines that differed in the expression of ACE2. As determined by FACS analysis, the expression level of ACE2 on the surface of the Vero cell lines E6, CCL-81, and RIE15 was characterized by the ratio 30:23:5 (Fig. 6A, supplemental material). Compared to Vero E6 (100%) the number of bound BHK-SΔ18 cells was reduced to about 85% and 22%, when the CCL-81 or RIE15 sublines of Vero cells were used for the binding assay (Fig. 6B, supplemental material). These results indicate that the binding of BHK-SΔ18 cells to Vero E6 cells is mediated by the S protein of SARS-CoV.

For quantitative evaluation of the binding, cells were detached by trypsin digestion, resuspended in PBS containing 0.5% bovine serum albumin (BSA) and subjected to flow cytometry. Using this assay, we analyzed the importance of cholesterol for the binding. Confluent Vero E6 cells were treated with mβCD followed by the addition of BODIPY FL C_{12}-labeled BHK-SΔ18 cells. The treatment of Vero E6 cells with mβCD inhibited the binding of BHK-SΔ18 cells to Vero E6 cells in a dose-dependent manner (Fig. 3B). At an mβCD concentration of 10 mM, binding was decreased to about 50% which is similar to the reduction of the infection rate observed with VSV-ΔG-S (Fig. 2A) and SARS-CoV (Fig. 3) at the same mβCD concentration. The detrimental effect of the cholesterol depletion on the binding capacity of BHK-SΔ18 cells was abolished by the addition of exogenous cholesterol (Fig. 3B). The treatment with cholesterol even resulted in a 2-fold increase in binding of S-expressing cells to receptor-expressing cells. MβCD or cholesterol treatment of parental BHK cells did not affect the unspecific binding to Vero E6 cells (data not shown). The cell-based binding data suggest that cholesterol is important for optimal interaction of the spike protein with the receptor ACE2. This assay allows multi-ligand interactions which may be facilitated by cellular receptors arranged in membrane microdomains. To determine whether the interaction of isolated S proteins with membrane-bound ACE2 is also cholesterol-dependent, we applied a binding assay with soluble S protein. Cholesterol-depleted or replenished Vero E6 cells were incubated with soluble S proteins followed by the quantification of bound protein (Fig. 4). Compared to the cell-based binding assay, binding of the soluble spike protein construct was not dependent on cholesterol; similar amounts of S protein were bound whether or not the cells were pretreated with mβCD and/or cholesterol comparable to control cells. To avoid the criticism that the soluble S protein is not functional or not properly folded we performed experiments showing that the S1-Fc construct used is recognized by an antibody directed against the S protein of SARS-CoV (Fig. 7A, supplemental material). Furthermore, we demonstrated that the soluble S protein binds to transfected BHK cells expressing ACE2 but not to non-transfected cells. Binding was prevented by an antibody directed against S protein (Fig. 7B, supplemental material).

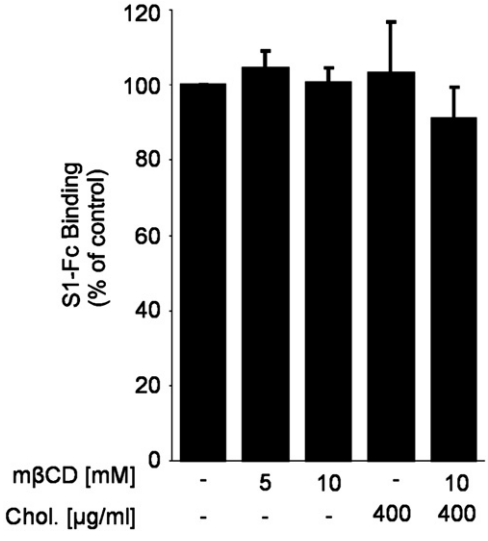

Fig. 4. Effect of cholesterol deletion on the binding of soluble spike glycoprotein to Vero E6 cells. For the binding assay with soluble SARS-CoV spike protein cholesterol-depleted or repleted Vero E6 cells were incubated with soluble S protein and bound S proteins were subsequently detected by using an anti-human FITC-conjugated secondary antibody followed by flow cytometry. The bars represent the mean ± standard deviation of 3 independent experiments.

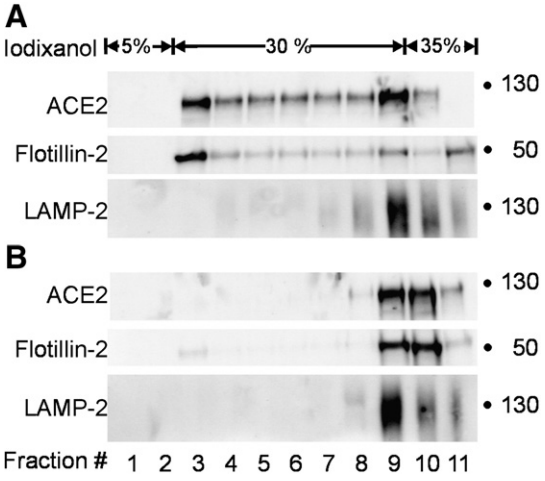

Fig. 5. Isolation of detergent-resistant membranes by step gradient centrifugation. Confluent Vero E6 cells were lysed in 1.0% Triton X-100 three to four days after initial seeding and cell lysates were subjected to step gradient ultracentrifugation. Fractions (1 ml) were collected from top to the bottom subjected to SDS-PAGE and analyzed by immunoblotting with antibodies directed against ACE2, Flotillin-2 and LAMP-2. The fractionation was performed with untreated cells (A) or cells that had been pretreated with mβCD (B). Blots show a representative experiment out of three.

ACE2 is localized in cholesterol-rich microdomains

As SARS-CoV entry is cholesterol-dependent and cholesterol is enriched in detergent-resistant membrane microdomains, one might expect that the cellular receptor for SARS-CoV, ACE2, is present in detergent-resistant membranes. However, it has been reported that, ACE2 is not located in detergent-resistant membranes (Warner et al., 2005; Li et al., 2007). On the other hand, Lu et al. (2008) recently detected ACE2 in the raft fraction of Vero E6. To clarify this discrepancy, we also analyzed whether ACE2 is resistant to solubilization by Triton X-100 at 4 °C. In contrast to previous reports (Warner et al., 2005; Li et al., 2007) we found that a substantial amount of ACE2 from Vero E6 cells was floating to the light fractions of the gradient where the detergent-resistant membranes are expected as indicated by the raft marker flotillin-2 (Fig. 5A). By contrast, the non-raft marker LAMP-2 was completely solubilized and recovered from the bottom fraction of the gradient. When mβCD-treated Vero E6 cells were subjected to such an analysis, ACE2 was detected only in the detergent-soluble fraction (Fig. 5B). This result indicates that a substantial portion of the SARS-CoV receptor ACE2 is associated with cholesterol-rich membrane microdomains that are resistant to detergent-solubilization at 4 °C. The same result was obtained when Caco-2 cells were analyzed (data not shown). The discrepancy between these results and previous reports will be discussed below.

Discussion

Our work extended the current knowledge about the cholesterol dependence of the SARS-CoV entry in the following way: (i) by

comparing infectious SARS-CoV and VSV pseudotypes containing the S protein of SARS-CoV we show that the cholesterol dependence is a property of the S protein and independent of other viral proteins, (ii) in contrast to two previous reports (Warner et al., 2005; Li et al., 2007) and in agreement with a recent report (Lu et al., 2008) we show for two cell lines that are sensitive to SARS-CoV that ACE2 is present in detergent-resistant membranes; (iii) for the first time we present experimental evidence indicating that cholesterol is required for efficient S-mediated binding to ACE2-containing cells.

The importance of cholesterol in the plasma membrane of the target cell has been shown for a number of viruses (Liao et al., 2001; Lu et al., 2002; Bender et al., 2003) including some coronaviruses (Nomura et al., 2004; Thorp and Gallagher, 2004; Choi et al., 2005; Imhoff et al., 2007; Li et al., 2007; Lu et al., 2008). Our results not just confirm this finding for SARS-CoV but go beyond this initial observation and provide additional data that contribute to a better understanding of the importance of cholesterol for infection by SARS-CoV.

We have demonstrated that cholesterol depletion affects not only infection by SARS-CoV but also S-mediated infection of VSV pseudotypes. In fact, the inhibitory effects observed in both systems are comparable. VSV itself is not impaired in its ability to infect cells that have a reduced content of cholesterol (Thorp and Gallagher, 2004; Imhoff et al., 2007). Based on these findings, the cholesterol dependence of SARS-CoV can be attributed to the S protein and appears to be unaffected by other viral proteins. Furthermore, our approach shows that cholesterol depletion reduces infectivity in a single replication cycle by about 50%.

The functions of the S protein in the early phase of infection are (i) binding to the cell surface receptor, and (ii) induction of the fusion between the viral and the cellular membrane. Our data obtained with the cell-based binding assay indicate that S-mediated binding to target cells is reduced by depletion of cholesterol from the ACE2-containing cells. On the other hand, the binding of soluble S protein was not affected. The differences can be explained by a multivalent interaction between the viral glycoproteins and cellular receptor molecules in the case of the cell-based binding assay which may be facilitated by the concentration of receptors in membrane microdomains. In contrast, soluble S proteins can only interact with individual ACE2 molecules and therefore, the binding efficiency is similar whether or not the receptor molecules are arranged in microdomains. Virus binding to cells does also allow multivalent interactions between the viral attachment protein and the cellular receptors. Therefore, arrangement of ACE2 in membrane microdomains would explain why cholesterol depletion from target cells reduces the infectivity of SARS-CoV by about 50%.

Our analysis of the surface expression indicates that cholesterol depletion does not reduce the amount of ACE2 protein on the surface of Vero cells. This finding argues against an explanation that quantitative differences in the availability of the cellular receptor account for the reduced binding efficiency. It has been reported that the amount of ACE2 expressed on the cell surface is reduced to some extent by cholesterol depletion (Li et al., 2007). The difference to our data may be due to different staining protocols. In our analysis, the anti-ACE2 antibodies were added prior to mβCD treatment whereas in the report by Li and co-workers, the antibodies were added after cholesterol depletion. We interpret these results such that cholesterol in the plasma membrane affects the conformation of ACE2 and thus the presentation of the antigenic epitopes. It should be noted that in a recent report the amount of ACE2 on the surface of Vero E6 cells was also not found to be reduced (Lu et al., 2008) which is in agreement with our data.

A straightforward explanation of the effect of cholesterol depletion on the binding of S protein would be that ACE2 is located in DRMs and that the concentration of this receptor in microdomains increases the efficiency of binding. The depletion of cholesterol from ACE2-expressing target cells might result in the dispersion of ACE2 molecules on the cell surface and abolish the spatial concentration of ACE2 in membrane microdomains. In fact, we found that a substantial amount of ACE2 from Vero E6 cells was colocalizing with flotillin-2, a marker for detergent-resistant membranes, and cholesterol depletion resulted in a reduction of ACE2 in the detergent-resistant membrane fraction after Triton X-100 solubilization. The same result was obtained when ACE2 from Caco-2 cells was analyzed (data not shown). The finding that ACE2 is located in DRMs is contradictory to previous reports that ACE2 is mainly detected in detergent-sensitive fractions (Warner et al., 2005; Li et al., 2007) but in agreement with Lu et al. (2008). The reason for this discrepancy with the former two reports may be the different experimental conditions. In one report, nonpolarized Chinese hamster ovary cells were analyzed (Warner et al., 2005), whereas the polarized cell lines Vero E6 and Caco-2 cells were used in our study. Furthermore, we determined the membrane association of endogenous ACE2, whereas others analyzed hamster cells overexpressing human ACE2 protein (Warner et al., 2005). In one report, the ACE2 distribution was also analyzed in Vero E6 cells (Li et al., 2007); however, it is not indicated at what time point after seeding the detergent treatment was carried out. In our experiments confluent Vero E6 cells were used three to four days after initial seeding; the differentiation state of the cells may influence the ACE2 distribution in the membrane environment. We found that endogenous ACE2 is located in detergent-resistant membranes of cells that are sensitive to infection by SARS-CoV. This location provides an explanation of the cholesterol dependence of the virus infection, most-likely during the binding of the virus to its receptor. A similar observation was reported for the binding of HIV-1 to dendritic cells (DC). Treatment of DCs with mβCD abolished virus binding at 4 °C indicating that DC-specific HIV-receptors are present in the cholesterol-enriched microdomains of the lipid bilayer (Gummuluru et al., 2003). As mentioned above, the importance of cholesterol-rich microdomains for infection by SARS-CoV may be a concentration effect on cellular receptor proteins. A clustering of ACE2 in certain areas of the membrane may allow multivalent binding of virus particles to the cell surface. In this way, microdomains may increase the efficiency of infection, but are not an absolute requirement for the entry process. This explanation is in agreement with the finding that cholesterol depletion reduces the susceptibility to infection but does not abolish it. Infectivity rates were reduced by about 50–60%. This may appear not to be a dramatic effect. However, infection of a host requires many replication cycles. Therefore, a virus that is able to produce a twofold higher number of infectious particles in one round of infection should have a huge advantage to survive in the long run. This is also evident from the other reports on the cholesterol dependence of SARS-CoV. These authors did not determine the infectivity of the mβCD-treated virus but the effect of mβCD treatment on a multi-cycle replication of SARS-CoV. Using this approach a 90% reduction of virus in the supernatant was found demonstrating the importance of efficient infection mediated by ACE2 in detergent-resistant membranes.

Materials and methods

Cells

All cell lines were propagated as adherent monolayer cultures in the presence of 5–10% heat-inactivated fetal calf serum (FCS) and a penicillin/streptomycin antibiotic cocktail. Baby hamster kidney (BHK21, German Collection of Microorganisms and Cell Cultures, Braunschweig, Germany) and Vero E6 cells (Collection of Cell Lines in Veterinary Medicine, Friedrich-Loeffler-Institute, Insel Riems, Germany) were grown in Eagle's minimal essential medium (EMEM), Vero CCL-81, Vero RIE15, and 293T cells were grown in Dulbecco's minimal essential medium (DMEM). BHK-G43 (Hanika et al., 2005)

and BHK-SΔ18 cells (stable transfectants as described below) were cultured in EMEM supplemented with the antibiotics zeocin (0.5 mg ml^{-1}) and hygromycin B (0.25 mg ml^{-1}).

Viruses

Replication-incompetent VSV with the G gene replaced by the eGFP gene (VSV-ΔG) was generated as described previously (Hanika et al., 2005). This approach was also used for the generation of SARS-CoV S-pseudotyped VSV (VSV-ΔG-S) as reported previously (Ren et al., 2006). Stock virus of the IBV strain Beaudette-US, and SARS-CoV strain Frankfurt were propagated on Vero CCL-81 and Vero E6 cells, respecitvely. VSV-ΔG-G-, VSV-ΔG-S- and IBV Beaudette-US viruses were stored at −80 °C and infectivity was determined by $TCID_{50}$ titration on BHK21, Vero E6 and Vero CCL-81 cells, respectively.

Virus infections

In general, untreated or cyclodextrin/cholesterol-treated cells were cultured on glass coverslips and washed prior to infection. VSV-ΔG viruses and IBV strain Beaudette were diluted in medium and ~10^2 infectious units were applied to the cells and allowed to bind at 37 °C for 1 h. After removal of the inoculum, medium containing 3% FCS was added to the cells. At 8 h p.i., the infected cells were washed once and fixed with 3% paraformaldehyde. VSV-ΔG virus infected cells were determined by counting eGFP-expressing cells. To monitor IBV infection, the fixed cells were permeabilized with 0.2% Triton X-100 and IBV antigen was stained by incubation with a rabbit serum raised against IBV strain Beaudette followed by incubation with FITC-conjugated secondary antibody. For infection with SARS-CoV (Frankfurt strain) Vero E6 cells were cultured in 6-well culture plates to reach confluency. The next day the cells were infected with a multiplicity of infection (MOI) of 0.0005. Virus was allowed to attach to the cells for 1 h at 37 °C. After having washed away unbound virus with PBS, cells were overlaid with DMEM containing 1% methylcellulose and cells were further incubated for 96 h. For visualizing plaque formation, cells were fixed with 4% paraformaldehyde followed by staining with crystal violet.

Baby hamster kidney cell line expressing SARS-CoV spike glycoprotein

A BHK21 cell line was generated that expresses the SARS-CoV S glycoprotein (BHK-SΔ18). The cell line was designed for the generation of viral pseudotypes containing the S proteins of SARS-CoV. Efficient pseudotyping was reported only for S constructs that lacked the carboxyterminal amino acids (Nie et al., 2004). Therefore, a mutant was generated with a deletion of the 18 carboxyterminal amino acids in the cytoplasmic tail of the S protein. For the generation of BHK-SΔ18 cells, the inducible mammalian GeneSwitch System (Invitrogen) was used. The following primers: 5′-TTTTGGATCCATCATGGATGCAATGAAGAGAGGGCTCTG-3′ and 5′-TTTTGAATTCTCACTTCAGGCAGCTGCAGCAGCTGGTCAT-3′ were designed to generate the truncated version of the SARS-CoV S protein by using a synthetic, codon-optimized sequence of the S gene (amino acid sequence is identical to strain BJ01, GenBank Accession No. AY278488) as a template. The BamHI/EcoRI digested and purified PCR product was inserted into the vector pGeneC to give pGeneC-SΔ18. The total open reading frame was sequenced and found to be correct. A cell line expressing the truncated SARS-CoV S protein was generated as described by the manufacturer. In brief, pGeneC-SΔ18/pSwitch-cotransfected BHK21 cells were cultured for 14 days in selection medium containing hygromycin B (500 μg ml^{-1}) and zeocin (1 mg ml^{-1}). Cell clones were isolated by limiting dilution and analyzed for mifepristone-induced SARS-CoV S expression by Western blotting and the production of VSV-ΔG-S pseudoparticles as described above. After a recloning step, one cell clone was selected and used throughout the study.

Cyclodextrin and cholesterol treatments of Vero cells

Methyl-β-cyclodextrin (mβCD, Cat. No. C-4555) and water-soluble cholesterol (Cat. No. C-4951) were obtained from Sigma-Aldrich. Vero CCL-81 or Vero E6 cells were treated with different concentrations of mβCD diluted in EMEM at 37 °C for 30 min. In cholesterol replenishment experiments, cells were first incubated with mβCD. After three washing steps cholesterol was diluted in serum-free EMEM and incubated with the cells at 37 °C for 30 min at a concentration of 100–400 μg ml^{-1}. For cholesterol measurement, the cells were washed with PBS, lysed in NP-40 lysis buffer and cholesterol levels were assayed using the Amplex Red Cholesterol Assay kit (Molecular Probes) following the manufacturers' protocol. Cell viability was assayed by using the WST-1 reagent (Roche). In brief, Cell Proliferation Reagent WST-1 was diluted 1:10 in medium and was then added to the cells. After incubation for 1 h at 37 °C, the absorbance was measured in an ELISA reader at 450 nm. In all experiments control cells were incubated with medium at 37 °C for the indicated time periods.

Binding assays and flow cytometry

For the cell-based binding assay BHK-SΔ18 cells were grown in 175 cm^2 culture flasks to 80% confluency. Culture medium was replaced with fresh medium containing 0.25 μg ml^{-1} BODIPY FL C_{12} (Molecular Probes), 5% FCS and 10^{-8} M mifepristone to induce S protein expression. After Accutase treatment (PAA Laboratories), the cells were resuspended in EMEM, counted and adjusted to 3×10^5 cells/ml. Vero E6 cells were incubated overnight in 24-well plates to confluent cell monolayers. Following cholesterol depletion/repletion Vero E6 cells were overlaid with 500 μl BHK-SΔ18 cell suspension for 2 h at 4 °C in the dark. After three washing steps with ice-cold PBS containing 0.5 M sodium chloride, binding of cells was visualized by fluorescence microscopy. For the quantification of Vero E6, BHK-SΔ18 cell–cell interaction, the cell mixture was detached, resuspended in PBS containing 1.0% BSA and subjected to flow cytometry on a Beckman Coulter Epics XL flow cytometer and analyzed using EXPO32 analysis software. To determine the specificity of the cell–cell interaction, BHK-SΔ18 cells were pre-incubated with anti-SARS rabbit serum diluted 1:50 followed by the cell overlay onto Vero E6 cells. BODIPY FL C_{12}-labeled BHK21 cells were used to determine unspecific binding. For the binding assay with soluble S protein, soluble Fc fusion proteins were transiently expressed in BHK21 cells, concentrated from culture supernatant by using CentriconPlus ultrafilters (Millipore), and incubated for 60 min on ice with cholesterol-depleted/repleted Vero E6 cells. Bound Fc fusion proteins were subsequently detected by using an anti-human FITC-conjugated secondary antibody (Dako) followed by flow cytometry.

Preparation of detergent-resistant membranes (DRM)

DRMs were prepared according to a published method (Castelletti et al., 2008) with modifications. All steps were carried out at 4 °C. Vero E6 cells were cultured in 60 mm culture dishes and were maintained for 3 days after reaching confluency. After washing with ice-cold PBS cells were scraped into 1 ml PBS containing 1.0% (w/v) TX-100 and Complete protease inhibitor cocktail (Roche Pharmaceuticals), homogenized by repeated passage through a 21-G needle and then maintained on ice for 2 h. A post-nuclear supernatant was prepared (7000 ×g, 15 min), the samples were diluted in iodixanol to a final concentration of 35% and 2 ml aliquots were transferred to SW-41 tubes. The samples were then overlaid with 30% (w/v, 8 ml) and 5% (w/v, 2 ml) on top of iodixanol in PBS. After centrifugation at 100,000 ×g for 18 h at 4 °C in a Beckman SW-41 rotor 1 ml fractions were harvested from the top to the bottom of the tube followed by separation under reducing conditions and the samples were then

analyzed for the protein content by western blotting. For the detection of ACE2 a goat anti-ACE2 polyclonal antibody (R&D System; 1:50) was used. The distribution of the raft marker protein flotillin-2 (BD Biosciences; 1:2000) and non-raft marker protein LAMP-2 (BD Pharmingen; 1:2000) was used as positive and negative controls, respectively.

Acknowledgments

Financial support was provided by funds from Deutsche Forschungsgemeinschaft (GRK745, He1168/12-1, and SFB621), the Sino-German Center for Research Promotion, and from the European Community (No. 511064). We are thankful to Gert Zimmer for providing the VSV pseudovirus system, to Christine Winter for anti-IBV rabbit serum, to Markus Eickmann for providing a rabbit serum against SARS-CoV, and to Stefan Pöhlmann for providing SARS-CoV S1-Fc fusion construct.

Appendix A. Supplementary data

Supplementary data associated with this article can be found, in the online version, at doi:10.1016/j.virol.2008.08.026.

References

Bender, F.C., Whitbeck, J.C., Ponce de Leon, M., Lou, H., Eisenberg, R.J., Cohen, G.H., 2003. Specific association of glycoprotein B with lipid rafts during herpes simplex virus entry. J. Virol. 77 (17), 9542–9552.

Castelletti, D., Alfalah, M., Heine, M., Hein, Z., Schmitte, R., Fracasso, G., Colombatti, M., Naim, H.Y., 2008. Different glycoforms of prostate-specific membrane antigen are intracellularly transported through their association with distinct detergent-resistant membranes. Biochem. J. 409 (1), 149–157.

Chazal, N., Gerlier, D., 2003. Virus entry, assembly, budding, and membrane rafts. Microbiol. Mol. Biol. Rev. 67 (2), 226–237.

Choi, K.S., Aizaki, H., Lai, M.M., 2005. Murine coronavirus requires lipid rafts for virus entry and cell–cell fusion but not for virus release. J. Virol. 79 (15), 9862–9871.

Enjuanes, L., Almazan, F., Sola, I., Zuniga, S., 2006. Biochemical aspects of coronavirus replication and virus–host interaction. Annu. Rev. Microbiol. 60, 211–230.

Garten, W., Klenk, H.D., 1999. Understanding influenza virus pathogenicity. Trends Microbiol. 7 (3), 99–100.

Gummuluru, S., Rogel, M., Stamatatos, L., Emerman, M., 2003. Binding of human immunodeficiency virus type 1 to immature dendritic cells can occur independently of DC-SIGN and mannose binding C-type lectin receptors via a cholesterol-dependent pathway. J. Virol. 77 (23), 12865–12874.

Hanika, A., Larisch, B., Steinmann, E., Schwegmann-Wessels, C., Herrler, G., Zimmer, G., 2005. Use of influenza C virus glycoprotein HEF for generation of vesicular stomatitis virus pseudotypes. J. Gen. Virol. 86, 1455–1465.

Imhoff, H., von Messling, V., Herrler, G., Haas, L., 2007. Canine distemper virus infection requires cholesterol in the viral envelope. J. Virol. 81 (8), 4158–4165.

Li, G.M., Li, Y.G., Yamate, M., Li, S.M., Ikuta, K., 2007. Lipid rafts play an important role in the early stage of severe acute respiratory syndrome-coronavirus life cycle. Microbes Infect. 9 (1), 96–102.

Liao, Z., Cimakasky, L.M., Hampton, R., Nguyen, D.H., Hildreth, J.E., 2001. Lipid rafts and HIV pathogenesis: host membrane cholesterol is required for infection by HIV type 1. AIDS Res. Hum. Retroviruses. 17 (11), 1009–1019.

Lu, X., Xiong, Y., Silver, J., 2002. Asymmetric requirement for cholesterol in receptor-bearing but not envelope-bearing membranes for fusion mediated by ecotropic murine leukemia virus. J. Virol. 76 (13), 6701–6709.

Lu, Y., Liu, D.X., Tam, J.P., 2008. Lipid rafts are involved in SARS-CoV entry into Vero E6 cells. Biochem. Biophys. Res. Commun. 369 (2), 344–349.

Marsh, M., Helenius, A., 2006. Virus entry: open sesame. Cell 124 (4), 729–740.

Nie, Y., Wang, G., Shi, X., Zhang, H., Qiu, Y., He, Z., Wang, W., Lian, G., Yin, X., Du, L., Ren, L., Wang, J., He, X., Li, T., Deng, H., Ding, M., 2004. Neutralizing antibodies in patients with severe acute respiratory syndrome-associated coronavirus infection. J. Infect. Dis. 190 (6), 1119–1126.

Nomura, R., Kiyota, A., Suzaki, E., Kataoka, K., Ohe, Y., Miyamoto, K., Senda, T., Fujimoto, T., 2004. Human coronavirus 229E binds to CD13 in rafts and enters the cell through caveolae. J. Virol. 78 (16), 8701–8708.

Popik, W., Alce, T.M., Au, W.C., 2002. Human immunodeficiency virus type 1 uses lipid raft-colocalized CD4 and chemokine receptors for productive entry into CD4(+) T cells. J. Virol. 76 (10), 4709–4722.

Ren, X., Glende, J., Al-Falah, M., de Vries, V., Schwegmann-Wessels, C., Qu, X., Tan, L., Tschernig, T., Deng, H., Naim, H.Y., Herrler, G., 2006. Analysis of ACE2 in polarized epithelial cells: surface expression and function as receptor for severe acute respiratory syndrome-associated coronavirus. J. Gen. Virol. 87 (Pt 6), 1691–1695.

Sieczkarski, S.B., Whittaker, G.R., 2002. Influenza virus can enter and infect cells in the absence of clathrin-mediated endocytosis. J. Virol. 76 (20), 10455–10464.

Simons, K., Ikonen, E., 1997. Functional rafts in cell membranes. Nature 387 (6633), 569–572.

Thorp, E.B., Gallagher, T.M., 2004. Requirements for CEACAMs and cholesterol during murine coronavirus cell entry. J. Virol. 78 (6), 2682–2692.

Warner, F.J., Lew, R.A., Smith, A.I., Lambert, D.W., Hooper, N.M., Turner, A.J., 2005. Angiotensin-converting enzyme 2 (ACE2), but not ACE, is preferentially localized to the apical surface of polarized kidney cells. J. Biol. Chem. 280 (47), 39353–39362.